Magnetohydrodynamic activity and energetic ions in fusion plasmas

Ya I Kolesnichenko[1], V V Lutsenko[1], V S Marchenko[1], A Weller[2], R B White[3], Yu V Yakovenko[1], K Yamazaki[4]

[1]Institute for Nuclear Research, Prospect Nauky 47, Kyiv, 03680, Ukraine
[2]Max-Planck-Institut für Plasmaphysik, D-17489 Greifswald, Germany
[3]Princeton Plasma Physics Laboratory, Princeton, New Jersey, 08543, USA
[4]Nagoya University, Furo-cho, Chikusa-ku, Nagoya 464-8603, Japan

Abstract. Selected issues of mutual influence of the energetic ions and collective phenomena in toroidal plasmas are considered. This includes peculiarities of energetic-ion-driven Alfvén instabilities in stellarators, fishbone instability and MHD activity during tangential neutral beam injection in tokamaks and spherical tori with the shearless core.

1. Introduction

Plasma in toroidal fusion devices is typically MHD active and contains energetic ions produced by neutral beam injection, fusion reactions, and acceleration during RF heating. Many important and interesting collective phenomena are associated with these ions (see, e.g., [1, 2]).

In particular, these are Alfvén instabilities caused by spatial inhomogeneity and/or velocity anisotropy of the energetic ions. Alfvén instabilities were observed in many experiments on tokamaks, stellarators, and spherical tori. They can have very different forms and consequences [3, 4, 5]. In stellarators, Alfvén instabilities have a number of peculiarities. Some of them were reviewed in Ref. [6]. In this paper, we concentrate on new results. In particular, new features of the high-frequency eigenmodes associated with the lack of the axial symmetry in stellarators and effects of the finite orbit width are reported.

Another important instability caused by the energetic ions is fishbone oscillations in tokamaks. The fishbone in the conventional case of $q < 1$ inside the $q = 1$ radius (q is the safety factor) and the shear $\hat{s} \equiv \mathrm{d}\ln q/\mathrm{d}\ln r \sim 1$ is typically an $m = n = 1$ rigid kink displacement of the plasma core, where m and n are the poloidal mode number and toroidal mode number, respectively [2]. We consider fishbones with completely different radial structure in systems with $q(r)$ close to unity or other low-order rationals in a wide core region surrounded by a region with large magnetic shear. This behavior of $q(r)$ is typical for spherical tori. In addition, this can be the case in tokamaks, in particular, in the ITER third operational scenario, in the so-called "hybrid" regime.

The energetic ions can stabilize sawtooth oscillations and other magnetohydrodynamic (MHD) events which are known to occur often in tokamak plasmas. The stabilizing effect can be due to trapped particles [7] and circulating ones [8]. Theoretical analysis of this phenomenon is usually relevant to plasmas with $\hat{s} \sim 1$. The

influence of the energetic ions on MHD activity of plasmas with the shearless core is not considered yet; it is known only that the trapped particles play a minor role in this case because the perturbed magnetic flux encircled by the precessional drift orbits vanishes in the limit of $1 - q \to 0$ [9]. This motivated us to consider the influence of circulating energetic ions on MHD activity in plasmas with the shearless core.

2. Alfvén instabilities in stellarators

2.1. Effects of fast-ion-orbit width and the mode width

The physical mechanism responsible for the destabilization of Alfvén eigenmodes by energetic ions is the resonant wave-particle interaction. The corresponding resonance can be obtained as follows. An equation describing the energy exchange between an energetic ion and an Alfvén wave is $\mathrm{d}\mathcal{E}/\mathrm{d}t = e\boldsymbol{v}_D \cdot \tilde{\boldsymbol{E}}$, where $\mathcal{E}$ is the particle energy, $\boldsymbol{v}_D$ is the drift velocity caused by the curvature and inhomogeneity of the magnetic field, $\tilde{\boldsymbol{E}}$ is the perturbed electric field. We take

$$\tilde{\boldsymbol{E}} = \sum_{m,n} \boldsymbol{E}_{m,n}(r) \exp(im\vartheta - in\varphi - i\omega t) \tag{1}$$

and expand the equilibrium magnetic field in a Fourier series as

$$B = \bar{B}\left[1 + \frac{1}{2}\sum_{\mu,\nu=-\infty}^{\infty} \epsilon_B^{(\mu\nu)}(r) \exp(i\mu\vartheta - i\nu N\varphi)\right], \tag{2}$$

where r is the radial coordinate defined by $\psi = \bar{B}r^2/2$ with ψ the toroidal magnetic flux and $\bar{B}$ the average magnetic field at the magnetic axis, ϑ and φ are the poloidal angle and toroidal angle, respectively, N is the number of the field periods. Then, considering the equation for $\mathrm{d}\mathcal{E}/\mathrm{d}t$ on the particle orbit, restricting ourselves to circulating particles, and neglecting the orbit width in the exponent (by taking $r = \mathrm{const}$, $\vartheta = \omega_\vartheta t + \vartheta_0$, $\varphi = \omega_\varphi t + \varphi_0$, where $\omega_\vartheta = \mathrm{const}$ and $\omega_\varphi = \mathrm{const}$ are the frequencies of the poloidal and toroidal motion of a particle, respectively, $\omega_\vartheta = \iota\omega_\varphi$, $\vartheta_0 = \mathrm{const}$, $\varphi_0 = \mathrm{const}$, and $\iota = q^{-1}$ the rotational transform), we obtain:

$$\frac{\mathrm{d}\mathcal{E}}{\mathrm{d}t} \sim \sum_{\mu,\nu,m,n} a^{(\mu\nu)} \exp[-i\omega t + i(m+\mu)\omega_\vartheta t - i(n+\nu N)\omega_\varphi t], \tag{3}$$

where $a^{(\mu\nu)}$ are some coefficients. It follows from equation (3) that an energetic ion can transfer a considerable part of its energy for a sufficiently long time interval Δt, $\Delta t \gg \max\{\omega_\varphi^{-1}, \omega_\vartheta^{-1}\}$, when the following resonance occurs:

$$\omega - (m+\mu)\omega_\vartheta + (n+\nu N)\omega_\varphi = 0. \tag{4}$$

In the case of the large-aspect-ratio tokamaks, $|\mu| = 1$, $\nu = 0$; therefore, for the well-circulating particles the only possible resonance is $\omega = (k_\parallel \pm \iota/R_0)v_\parallel$, where $k_\parallel = (m\iota - n)/R_0$, $v_\parallel$ is the particle velocity along the magnetic field, R_0 is the radius of the magnetic axis. In particular, this leads to the resonance velocities $v_\parallel^{\mathrm{res}} = -\sigma_k v_A(r_*)$ and $v_\parallel^{\mathrm{res}} = \sigma_k v_A(r_*)/3$ [v_A the Alfvén velocity, r_* the radius of the mode localization, and $\sigma_k = \mathrm{sgn}(k_\parallel)$] for the well-localized Toroidicity-induced Alfvén Eigenmodes (TAE) having $\omega = \iota_* v_A(\iota_*)/(2R_0)$ with $\iota_* = \iota(r_*)$.

Finite mode width affects this result. For instance, it can provide the interaction of the ions with the velocity slightly smaller than v_A. This is of importance when the

injection velocity, v_α, is less than v_A, so that the injected ions cannot interact with the waves through the resonance $|v_\parallel| = v_A$ in the local approximation, but the drive through the resonance $|v_\parallel| = v_A/3$ is weak. This explains an LHD experiment where the finite width of the mode provided the resonance $|v_\parallel| \approx v_A$ for the even mode but not for the odd mode (see [6] and references therein). As a result, the growth rate of the even-mode instability (γ_{even}) well exceeded that of the odd-mode instability (γ_{odd}): $\gamma_{\text{even}}/\gamma_{\text{odd}} \approx 10$, $\gamma_{\text{even}}/\omega \approx 20\beta_\alpha(0)$, with β_α the beam beta.

It follows from equation (4) that the presence of the non-axisymmetric harmonics in the magnetic field ($\nu \neq 0$) leads to additional resonances (see [6] and references therein).

Now we take into account the particle orbit width, Δ_b [in which case $r = \bar{r} + \Delta_b \cos\vartheta$, $\vartheta = \vartheta_0 + \omega_\vartheta t - (\epsilon'_t/\epsilon_t)\Delta_b(\sin\vartheta - \sin\vartheta_0)$, $\varphi = \varphi_0 + \omega_\varphi t$], where $\epsilon_t = -\epsilon_B^{(10)} > 0$ is the toroidal harmonic, $\epsilon'_t = \mathrm{d}\epsilon_t/\mathrm{d}r$. Then we can write

$$E_{m,n}[r(\vartheta)] = \sum_l E_{m,n,l}(\bar{r})e^{il\vartheta}, \quad e^{i\zeta \sin\vartheta} = \sum_q J_q(\zeta)e^{iq\vartheta}, \tag{5}$$

with $\zeta = (m + l + \mu)\Delta_b\epsilon'_t/\epsilon_t$. This leads to the resonance

$$\omega R_0 = [k_\parallel R_0 + (\mu + l - q)\iota - n - \nu N]v_\parallel^{\text{res}}. \tag{6}$$

Equation (6) shows that the finite orbit width leads to new resonant velocities, which, however, weakly contribute to the energy exchange when $\zeta \gg 1$, i.e., when the orbit width well exceeds the mode width.

A theory taking into account effects of finite Δ_b in stellarators was developed in Ref. [10]. It was also applied to an experiment on Wendelstein 7-AS (the shot #34723), where the Alfvénic activity had a bursting character, being strongest at the end of each burst and characterized by frequency chirping down (from ~ 65 kHz to ~ 45 kHz). A detailed study explained this [10, 11]. It was found that finite orbit width triggers a weak instability (by providing the resonance interaction at the frequency ~ 65 kHz), which was identified as Non-conventional Global Alfvén Eigenmode (NGAE), i.e., the mode with a frequency above the Alfvén continuum (in contrast to the well-known GAE modes with the frequency below the continuum). In addition, it was concluded that the finite orbit width weakens the strong instability at the end of the instability burst by reducing the wave-particle energy exchange due to $\zeta > 1$.

2.2. Poloidal structure of the high-frequency Alfvén modes

The Alfvén continuum (AC) in stellarators in the high frequency range [in the range of the helicity-induced gaps ($\mu \neq 0, \nu = 1$) and the mirror-induced gap ($\mu = 0, \nu = 1$)] is compressed by wide gaps into extremely thin threads, as shown for a W7-AS shot in figure 1. Let us consider eigenmodes in this part of the frequency spectrum.

Applying the ballooning formalism described in [12] to the Alfvén wave equation [13], we obtain the following equation, which determines the scalar potential of the electromagnetic field of the eigenmode (Φ) along a field line:

$$\frac{\mathrm{d}}{\mathrm{d}\varphi}\left(D\frac{\mathrm{d}\Phi}{\mathrm{d}\varphi}\right) + \Omega^2\frac{D}{h_B^4}\Phi = 0, \tag{7}$$

where

$$D = h_g^{\vartheta\vartheta} + 2(\varphi - \varphi_k)\hat{s}\iota h_g^{\psi\vartheta} + (\varphi - \varphi_k)^2\hat{s}^2\iota^2 h_g^{\psi\psi}, \tag{8}$$
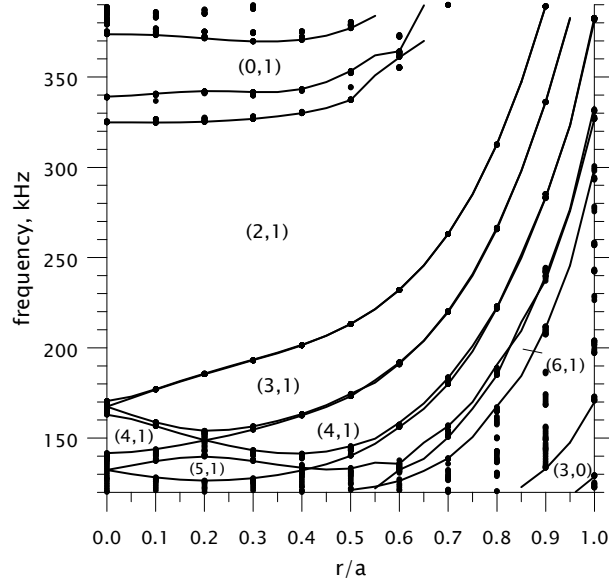
Figure 1. High frequency part of Alfvén continuum calculated with the code COBRA [13] in W7-AS shot No. 56936. Notations: dots, the AC at certain radial points; solid lines, boundaries of some gaps. The gaps are labelled by the corresponding coupling numbers (μ, ν).

$\Omega = \omega R_0 / \langle v_A \rangle$, $\langle \ldots \rangle = \oint \mathrm{d}\vartheta \, \mathrm{d}\varphi \, (\ldots)/(4\pi^2)$, $h_B = B/\langle B \rangle$, $h_g^{\psi\psi} = g^{\psi\psi}/\langle g^{\psi\psi} \rangle$, $h_g^{\vartheta\vartheta} = g_\perp^{\vartheta\vartheta}/\langle g_\perp^{\vartheta\vartheta} \rangle$, and $h_g^{\psi\vartheta} = g^{\psi\vartheta}/(\langle g^{\psi\psi} \rangle \langle g_\perp^{\vartheta\vartheta} \rangle)^{1/2}$ are normalized metric tensor components, $g_\perp^{\vartheta\vartheta} = g^{\vartheta\vartheta} - (b^\vartheta)^2$; g^{ij} with $i, j = \psi, \vartheta, \varphi$ are the components of the contravariant metric tensor; b^ϑ denotes the corresponding contravariant component of $\boldsymbol{b} \equiv \boldsymbol{B}/B$, prime means differentiation in ψ, φ_k is a standard parameter of the ballooning formalism, which characterizes the transversal wave number.

We consider the frequency range of two adjacent helicity-induced gaps with the numbers $(\mu, 1)$ and $(\mu + 1, 1)$ and assume for simplicity that each of the dimensionless coefficients $h_g^{\psi\psi}$, $h_g^{\vartheta\vartheta}$, $h_g^{\psi\vartheta}$, and h_B includes only the corresponding two harmonics proportional to $\exp(i\mu\vartheta - iN\varphi)$ and $\exp[i(\mu + 1)\vartheta - iN\varphi]$. The substitution $\Phi = D^{-1/2}\hat{\Phi}$ transforms equation (7) into a Schrödinger-type equation:

$$\frac{\mathrm{d}^2\hat{\Phi}}{\mathrm{d}\varphi^2} + \Omega^2 U(\varphi)\hat{\Phi} = 0, \tag{9}$$

with the potential U schematically shown in figure 2 for the case of $N \gg \iota$. The potential possesses three characteristic scales in φ. The smallest one, $\Delta\varphi \sim 2\pi/N$, is approximately the period of each harmonic. The second one, $\Delta\varphi \sim 2\pi/\iota$, is the period of the beatings associated with the presence of two harmonics with close periods along the field lines. The third one, $\Delta\varphi \sim 2/(\iota\hat{s})$, is the characteristic scale that usually appears in the ballooning theory. Averaging over the fast oscillations shows that the eigenmodes of equation (9) are localized in the "pockets" of the envelope, which are the places where the net amplitude of the two harmonics is minimum. For instance, the Helicity-induced Alfvén Eigenmodes (HAEs) produced by the Fourier harmonics with $(\mu, \nu) = (2, 1)$ and $(3, 1)$ are typically localized at the inner circumference of the torus, which is determined by the signs of the corresponding harmonics of the
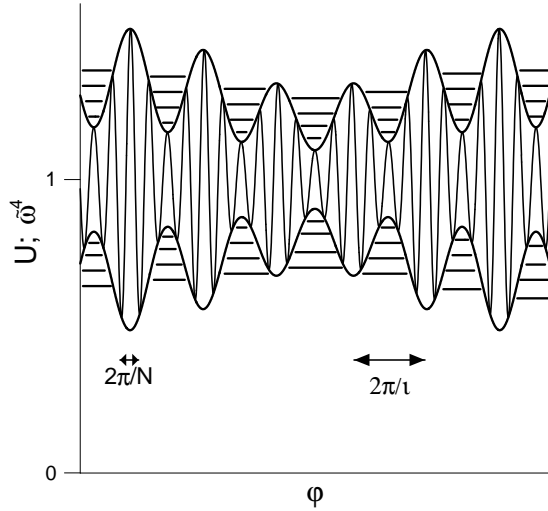
Figure 2. Sketch of the potential U in equation (9) and the bounded states. Thin curve, U; bold curves, the envelopes of U; horizontal lines, the frequencies $[\tilde{\omega} = (2/N)(R_0/v_A)\omega]$ and the localizations of eigenmodes.

configuration (in general, other localizations are also possible, see [14]).

Note that the nature of this "anti-ballooning" structure of the considered HAEs differs from the nature of the anti-ballooning structure of the odd TAE. The latter results from approximate vanishing of the sum of two principal harmonics of the mode at $\vartheta = 0$. In contrast to this, the considered HAEs are poloidally inhomogeneous because they are evanescent near the outer circumference of the torus. This implies that the mode consists of many Fourier harmonics (much more than two) and it is much stronger localized poloidally. This conclusion can be relevant also to the mirror-induced Alfvén eigenmodes (MAE).

The presented results may explain an experimental observation of poloidally inhomogeneous Alfvénic activity in W7-AS. In this experiment, the intensity of some spectral lines in the range of $200 - 400 \, \text{kHz}$ (which corresponded to HAE frequencies) was much higher on the Mirnov coils located at the inner circumference of the torus than on the coils at the outer circumference (see [14]).

3. Interchange and infernal fishbone modes

In the case of the conventional $m = n = 1$ fishbone instability associated with trapped particles [2], there are two radial points of local Alfvén resonance, $r_{\text{res}}^{(1)}$ and $r_{\text{res}}^{(2)}$. Both these points are located close to the $q = 1$ radius, $r_{\text{res}}^{(1)} = r_s - \Delta$ and $r_{\text{res}}^{(2)} = r_s + \Delta$, with $\Delta \ll r_s$ and r_s is defined by $q(r_s) = m/n$. The small magnitude of Δ is explained by the fact that $\omega/\omega_{\text{AC}}(r = 0) \ll 1$, where $\omega_{\text{AC}}(r) \approx |\iota(r) - 1|v_A(r)/R_0$ is the Alfvén continuum frequency. This implies that the finite frequency of the EPM mode, $\omega \sim \omega_D^t$, with ω_D^t the precession frequency of the trapped particles, affects the structure of MHD perturbations with $\omega = 0$, i.e., the internal kink mode, only in the region where the mode amplitude is rapidly decreasing. However, when B is low, and/or q is close to unity inside the $q = 1$ radius, the ratio $\omega/\omega_{\text{AC}}(0)$ is not small
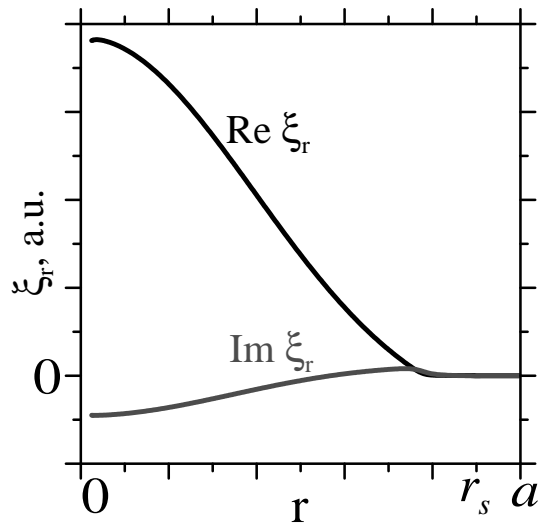
Figure 3. Radial structure of a fishbone mode (ξ_r is the radial plasma displacement) in the NSTX spherical torus for $\beta_\alpha(r) = \beta_0(1 - r^2/a^2)^2$, $\beta_0 = 8.82 \times 10^{-3}$. The calculated mode frequency is $\omega/\omega_D^t = 0.485$, which corresponds to $\omega/\omega_{AC}(0) = 0.998$, and the growth rate is $\gamma/\omega_D^t = 0.01$. The parameters used are: $A = 1.27$, $r_s/a = 0.87$, $q = 0.8$ for $r < r_c$, and $q = 0.8 + [1.9(r - r_c)/r_c]^{10}$ for $r > r_c$ with $r_c = 0.6a$, $a = 67$ cm.

because $\omega/\omega_{AC}(0) \propto \omega_D^t/\omega_{AC}(0) \propto (\iota_0 - 1)^{-1}B^{-2}$, with $\iota_0 = \iota(r = 0)$. Because of this, $r_{\text{res}}^{(2)}$ is shifted to the right, where the mode amplitude is much smaller than that at $r = 0$, whereas the resonance point $r_{\text{res}}^{(1)}$ may disappear. In this case, the structure of the ideal MHD perturbations with $\omega = 0$ is again not essentially affected by the energetic ions, but this structure has nothing to do with the rigid kink displacement, see figure 3 [15]. This result is not surprising: it is known that the eigenfunction of the $m = n = 1$ MHD mode at small shear has convective, cellular character, in contrast to the rigid kink displacement in the finite shear case [16]. We refer to the mode with the structure similar to that shown in figure 3 as the "interchange fishbone".

The non-rigid character of perturbations in low-shear systems is especially important when the energetic-ion population consists of circulating particles. In this case, it provides a strong energy exchange between the energetic ions and perturbations through the resonance $\omega = k_\parallel v_\parallel$ in a wide region (rather than in the region $r_s - \Delta_b < r < r_s$, which is the case when the mode represents a rigid kink displacement [17]). Moreover, due to this resonance a possible mode frequency is $\omega \sim k_\parallel(0)v_\alpha$ and, thus, $\omega > \omega_A(0)$ when $v_\alpha > v_A$, which implies that the Alfvén resonance points are located at the periphery.

A detailed study shows that the threshold beta of the circulating energetic ions, β_α^{th}, for which this instability can arise is rather small. Typically, β_α^{th} is of the order of several per cent in tokamaks and about 10^{-3} in spherical tori.

The resonance $\omega = k_\parallel v_\parallel$ can lead also to EPM fishbones with $m \neq 1$, $n \neq 1$ in low-shear core plasmas [18]. We refer to this instability as "infernal fishbones", taking into account that MHD modes in plasmas with shearless core are called "infernal" [19]. These fishbones are actually an EPM Alfvén instability with the frequency below that of TAE modes. They differ from another mode in the Alfvén continuum region,
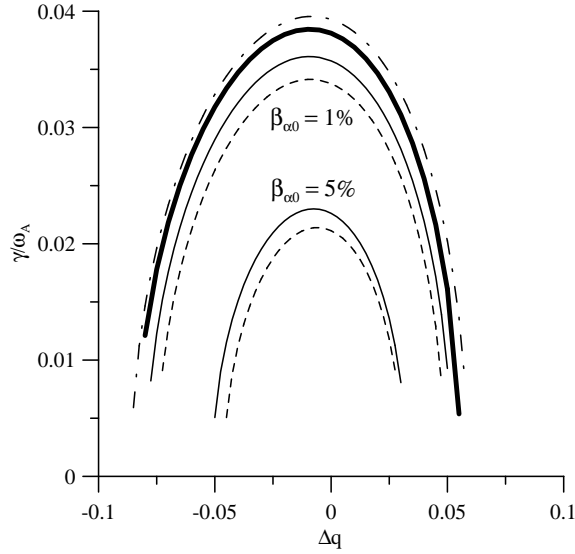
Figure 4. Dependence of the growth rate of the quasi-interchange mode on the central safety factor q_0 ($\Delta q = 1 - q_0$) without fast ions (thick solid line) and in the presence of these ions with $\beta_\alpha(0) = 1\%$ and 5%. Dashed/dash-dotted lines correspond to co/counter-injected ions. The following parameters were used: $a/R_0 = 0.3, \beta_0 = 0.1, l_1 = 2, l_2 = 4, q_a = 4, r_0/a = 0.5, v_\alpha/(a\omega_B) = 0.05$ with ω_B the ion gyrofrequency.

GAE, whose frequency is determined by the bulk plasma and lies below the Alfvén continuum branch corresponding to a dominant Fourier harmonic of the mode (the GAE frequency intersects the Alfvén continuum of satellite harmonics only).

The considered instabilities involve most energetic ions, $\mathcal{E} \lesssim \mathcal{E}_\alpha$, with $\mathcal{E}_\alpha$ the injection energy. Therefore, they may be responsible for strong drops of the neutron emission observed in NSTX during fishbones with multiple mode numbers, $n = 1 \div 4$ [20]. In this experiment, the modes with higher n had higher frequencies, which agrees with the theory prediction, $\omega \sim n(\iota_0 - 1)v_A/R_0$ for $n = m$.

4. Stabilization of sawteeth in low-shear core tokamaks by circulating energetic ions

Like in Sec. 3, here we consider an axisymmetric configuration with shearless plasma core and strong shear at the periphery but, in contrast to Sec. 3, here we are interested in perturbations with vanishing frequency. We use the energy functional, $\delta\mathcal{E}$, given by

$$\delta\mathcal{E} = \frac{R}{\pi^2 \bar{B}^2} \left[\delta W_{MHD} + \delta W_f + \delta W_k(\omega = 0)\right] + \frac{\gamma^2}{\omega_A^2} \frac{1}{2\pi^2 R} \int d^3 r |\boldsymbol{\xi}|^2, \qquad (10)$$

where δW_{MHD} is the ideal MHD potential energy [21] extended to include the effect of the fast ions on the Shafranov shift, δW_f and δW_k are the fluid response of energetic ions and their kinetic response, respectively, the last term represents the kinetic energy, $\omega_A = v_A/R_0$, $\boldsymbol{\xi}$ the plasma displacement, and $\gamma = \mathrm{Im}\,\omega$.

We assume that $\beta(r) \equiv 8\pi p/\bar{B}^2 = \beta_0 \left(1 - r^2/a^2\right)^{l_1}$, $\beta_\alpha(r) \equiv 8\pi p_\alpha/\bar{B}^2 = \beta_{\alpha 0} \left(1 - r^2/a^2\right)^{l_2}$, $l_2 > l_1$, and $q(r) = q_0$ for $0 \leq r \leq r_0$, $q(r) = q_0 - (q_a - q_0)(r -$

$r_0)^2/(a - r_0)^2$ for $r_0 \leq r \leq a$, a is the plasma radius. With these assumptions, the Euler equations for the energy functional were solved numerically, neglecting δW_k [$\delta W_k(\omega = 0)$ is small in the shearless case]. The results are shown in Fig. 4. We observe that the fast ions produce a stabilizing effect in the case of co-injection and balanced injection, the effect being sufficiently strong when q_0 is not too close to unity. The stabilization (destabilization) by co- (counter-) injected ions is due to the fact that the radial displacement, $\xi_r(r)$, of the dominant $m = 1$ harmonic is a monotonically decreasing function (in contrast to the internal kink mode): the co- (counter-) injected ions with their orbits shifted outward (inward) "feel" smaller (larger) perturbation when passing through the region with unfavourable curvature.

5. Summary and conclusions

We revealed that the high-frequency Alfvén eigenmodes (HAEs and MAEs) in stellarators can be localized at the inner circumference of the torus and showed that the finite orbit width of fast ions can lead to additional resonant velocities playing an important role in a W7-AS experiment. We predicted the existence of new fishbone modes of the EPM type and found the stabilizing influence of the beam ions on sawtooth instability in axisymmetric devices with shearless core and strong shear at the periphery in the cases of co-injection and balanced injection.

Acknowledgments

[1] Kolesnichenko Ya I 1980 *Nucl. Fusion* **20** 727
[2] White R B 2001 *The Theory of Toroidally Confined Plasmas* (London: Imperial College Press)
[3] Wong K L 1999 *Plasma Phys. Control. Fusion* **41** R1
[4] Weller A *et al* 2001 *Phys. Plasmas* **8** 931
[5] Toi K *et al* 2004 *Plasma Phys. Control. Fusion* **46** S1
[6] Kolesnichenko Ya I *et al* 2004 *Fusion Sci. Technol.* **46** 54
[7] Campbell D J *et al* 1988 *Phys. Rev. Lett.* **60** 2148
[8] Kramer G J *et al* 2000 *Nucl. Fusion* **40** 1383
[9] Porcelli F *et al* 1992 *Phys. Fluids* B **4** 3017
[10] Kolesnichenko Ya I *et al* 2006 *Nucl. Fusion* **46** 753
[11] Kolesnichenko Ya I *et al* 2005 *Phys. Rev. Lett.* **94** 165004
[12] Dewar R L and Glasser A H 1983 *Phys. Fluids* **26** 3038
[13] Kolesnichenko Ya I *et al* 2001 *Phys. Plasmas* **8** 491
[14] Yakovenko Yu V *et al* 2006 *Proc. 13th Int. Congr. on Plasma Physics (Kiev, Ukraine, 22–26 May 2006)*, Report B022p, to be published.
[15] Kolesnichenko Ya I *et al* 2004 *Fusion Energy 2004, 20th IAEA Fusion Energy Conf. (Vilamoura)* IAEA-CSP-25/CD, Report TH/P4-42 (on CD-ROM)
[16] Wesson J A 1986 *Plasma Phys. Control. Fusion* **28** 243
[17] Betti R and Freidberg J P 1993 *Phys. Rev. Lett.* **70** 3428
[18] Marchenko V S *et al* 2005 *9th IAEA Technical Meeting on Energetic Particles in Magnetic Confinement Systems, Takayama, Japan*, Paper OT-08
[19] Manickam J 1987 *Nucl. Fusion* **27** 1461.
[20] Fredrickson E D *et al* 2003 *Phys. Plasmas* **10** 2852
[21] Waelbroeck F L and Hazeltine R D 1998 *Phys. Fluids* **31** 1217